Surpact

A SMOS Surface Wave Rider for Air-Sea Interaction

BY GILLES REVERDIN, SIMON MORISSET, DENIS BOURRAS, NICOLAS MARTIN, ANTONIO LOURENÇO, JACQUELINE BOUTIN, CHRISTOPHE CAUDOUX, JORDI FONT, AND JOAQUÍN SALVADOR

ABSTRACT. A new small wave rider called Surpact was developed for air-sea investigations. It was designed to attach to a drifter or a mooring and to float upon the surface waves in order to measure sea state and atmospheric sea level pressure as well as temperature and salinity at a small fixed depth from the surface. Wind speed is derived from Surpact sea state measurements, and the data are calibrated with co-located Special Sensor Microwave Imager Sounder (SSMIS) wind retrievals during a four-month deployment in the North Atlantic subtropics. Individual 15-minute wind estimates present a root mean square difference on the order of 15% with the SSMIS wind retrievals for wind speeds less than 12 m s^{-1}. The wind retrievals might lag the actual wind changes for moderate to strong winds by an hour. This article discusses the accuracy of these wind retrievals based on in situ data collected during the Strasse cruise in August and September 2012. Temperature and salinity data are also examined. The authors find, under some sunny conditions, radiative warming of the temperature probe reduces the accuracy of some of the daytime temperature data and also affects corresponding salinity estimates. Nonetheless, small realistic daily cycles of near-surface salinity (0.01 psu amplitude) were observed. Also, examples of wind time series collected during salinity drops caused by rainfall during late 2012 in the North Atlantic subtropics indicate no intensification of wind during these rain events.

INTRODUCTION

Surpact, a novel surface wave rider, was explicitly designed to measure temperature (T) and salinity (S) 4 cm below the sea surface, as well as sea state (and thus the inferred wind speed) and barometric pressure, reporting values every 15 minutes for 150 days. The data collected by Surpact will allow insight into the air-sea dynamics of haline evolution very close to the sea surface and provide better ground truthing of salinity derived from satellite radiometer measurements.

Near-surface diffusive processes and surface freshwater fluxes create a haline skin layer, typically less than 0.1 mm thick (Zhang and Zhang, 2011), that lies very near the surface. Salinity contrast across this thin layer can be greater than 0.1 psu in the presence of evaporation (Yu, 2010). The layer thickness of interest for ocean salinity and global water cycle studies is wider than the skin layer, so this surface skin layer is generally not measured. We refer to the salinity just below the skin layer as "subsurface salinity."

At a depth that is typically 1 m or more, salinity is less influenced by high-frequency variability (diurnal or higher). This "foundation salinity" is more typical of what has been historically measured through collection of surface samples by ships and salinity drifters, and these data are used to detect signatures associated with known modes of climate variability (Reverdin, 2010, in the North Atlantic; Cravatte et al., 2009, and Singh et al., 2011, in the tropical Pacific). These measurements usually provide a good proxy for mixed-layer salinity, and their variability has been related to the ocean water cycle, ocean circulation, and vertical mixing processes (Foltz and McPhaden, 2008; Schmitt, 2008; Yu, 2011; Bingham et al., 2010, 2012). Bingham et al. (2002) commented that the distribution of these near-surface salinity measurements is often non-Gaussian, which is to some extent related to air-sea freshwater fluxes, in particular, rainfall. Indeed, a study based to a large extent on Argo float vertical profiles (Henocq et al., 2010) indicated that vertical salinity differences higher than 0.1 psu between 1 m and 10 m depth are observed in the three tropical oceans, in particular, between 0° and 15°N, coinciding with high precipitation rates. Other studies based on mooring data (Cronin and McPhaden, 1999) or on drifter data (Reverdin et al., 2012) have also identified near-surface stratification related to tropical rainfall.

Satellite remote sensing by L-band frequency radiometry can be used to estimate salinity in a surface layer on the order of 1 cm thick (Swift, 1980), and subsurface salinity usually meets this criterion. SMOS (European Space Agency/Soil Moisture and Ocean Salinity; Font et al., 2010) and Aquarius/SAC-D (Lagerloef et al., 2012) satellite missions now provide observations of subsurface salinity. After correcting SMOS brightness temperatures using nonsea sources, SMOS-derived sea surface salinity (SSS) reproduces expected SSS variations at large scales (Font et al., 2013), but its accuracy as well as the accuracy of Aquarius retrievals are still subject to large uncertainties that require ground truth data for validation. Because the layer that the L-band measures is much thicker than the salinity skin-depth layer (Zhang and Zhang, 2012), the issue of validating/interpreting these satellite data with in situ observations involves not so much the issue of the skin layer, but that of subsurface stratification between 1 cm depth and the few decimeters to meters where most in situ observations are collected. For example, low values of SMOS salinity retrievals in rainfall areas have been attributed to such stratification (Boutin et al., 2012).

In order to better document the variability of subsurface salinity, some surface drifters in the last 10 years have been equipped with Sea-Bird conductivity/temperature (C/T) sensors attached near 50 cm depth (Reverdin et al., 2007, 2012). A difficulty with the data has been

Gilles Reverdin *(reve@locean-ipsl.upmc.fr) is Director of Research, LOCEAN/Institut Pierre Simon Laplace (IPSL), Paris, France.* **Simon Morisset** *is an engineer at LOCEAN/IPSL, Paris, France.* **Denis Bourras** *is a researcher at LATMOS/IPSL, Guyancourt, France.* **Nicolas Martin** *is an engineer at LOCEAN/IPSL, Paris, France.* **Antonio Lourenço** *is an engineer at LOCEAN/IPSL, Paris, France.* **Jacqueline Boutin** *is Director of Research at LOCEAN/IPSL, Paris, France.* **Christophe Caudoux** *is an engineer at LATMOS/IPSL, Guyancourt, France.* **Jordi Font** *is Research Professor, Institut de Ciències del Mar/Consejo Superior de Investigaciones Científicas (ICM/CSIC), Barcelona, Catalunya/Spain.* **Joaquín Salvador** *is an engineer at ICM/CSIC, Barcelona, Catalunya/Spain.*

that temperature and haline stratification across the top ocean layer can result in salinity errors because C and T measurements are not collected at the same depth. Furthermore, when a drogued drifter plunges into the waves, it induces mixing as well as uncertainty in the measurement's depth. Another limitation of these measurements is not knowing sea state, wind, and rain associated with them. Initially, we developed light "Surplas" floats to measure T and S near 17–20 cm depth. They alleviate some of the concerns, but C and T were still not measured at exactly the same depth. Furthermore, they do not provide sea state/wind measurements.

In this paper, we present developments associated with our new sensor package, Surpact. Prototypes attached to a mooring were tested close to the coast from April to June 2012 near Banyuls Observatory (Banyuls, France), and later during the Strasse cruise in the subtropical North Atlantic. We first present an overview of the float and its instrumentation. We then discuss how we estimate wind speed from Surpact 30798 sea state measurements made in the subtropical North Atlantic for 100 days, from September 9, 2012, to December 17, 2012 (30798 stopped transmitting on January 18, 2013), and how we calibrate these data based on co-located Special Sensor Microwave Imager Sounder (SSMIS) measurements. We then present ground truthing of the Surpact wind, temperature, and salinity estimates using data collected during the Strasse cruise in the subtropical North Atlantic between August 16 and September 14, 2012. We illustrate associated T and S variability during a few daily cycles and present estimates of wind during a few rainfall events recorded by the float during the 100-day period.

SURPACT DESIGN

The Surpact wave rider is composed of a floating annular ring (28 cm diameter) with a rotating axis across it to which the instrumented tag is attached (Figure 1). The axis across the tag is designed so that the tag remains nearly horizontal during its drift in waves with wave crests parallel to the axis. Its top surface floats an average 0.5 cm above the surface. This tag was inspired by the instrumentation placed on sea mammals to provide oceanographic data such as T, S profiles (Roquet et al., 2011). The tag transmits reduced data through the Argos system, and the full data can be internally recorded and transferred through Bluetooth upon recovery. The tag is equipped with Valport C/T sensors that remain 4–5 cm below the sea surface (we refer to this T measurement as T_c). The C-cell is an open inductive cell, and its tank tests show that it is not affected by close objects or by the sea surface, even with fairly strong waves. The measurement (we used it at 0.5 or 1 Hz sampling) is sensitive to bubbles and to tag motions, but their effect on C is reduced by considering the 80th upper percentile of data collected for

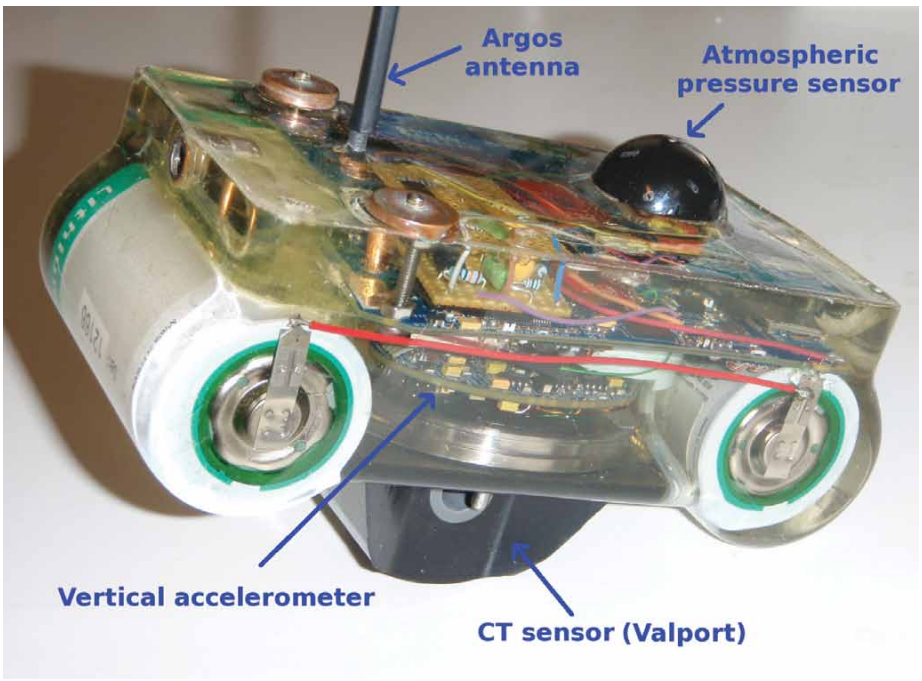

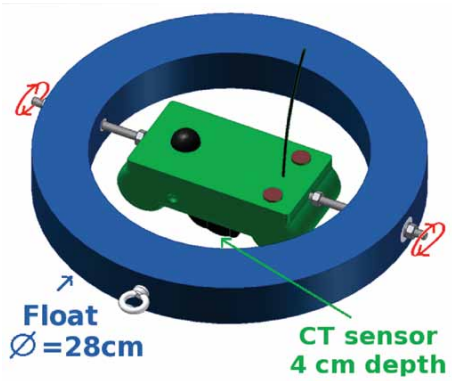

Figure 1. (left) Photograph of the Surpact tag. (above) Schematic of the float.

20 seconds. This was validated both in the tank and during a week of tests at sea west of Brittany in September 2011. (However, we recently found that this technique leaves some noise in a well-formed sea [up to 0.01 psu], and results are better when considering a 1 minute period). We associate C with the corresponding temperature measurement (this could induce a very small negative T bias during nighttime, based on some of the high-frequency data recorded during Strasse cruise deployments). The tag is also equipped with a three-component accelerometer and an atmospheric pressure (sea level pressure, or SLP) sensor on top of it under a holey semispherical cover with an associated temperature sensor (T_{slp}).

Because of the resin in which the tag is molded, a thermistor measures the temperature of the tag as well. The top of the sensor is then painted white before deployment to avoid having the sun directly heat the tag. Laboratory tests showed that internal tag temperature influences T_c. They showed that for an 8°C warming at the top of the tag in the middle of the day (as measured by T_{slp}), T_c increased by only 0.01°C. This small effect is corrected based on T_{slp} (without introducing a lag). However, we also found that the sun can still heat the tag base and thermistor through the semi-transparent side faces of the tag. Thus, if the sun shines obliquely, for example, when the tag moves with the waves or the sun's elevation is low (in the direction of the sensor), there is an additional error in T_c, which can be larger than 0.01°C. As C and T_c are used to estimate salinity, this warming also affects the estimated S. We recognized this issue occasionally during Surpact deployments in the summer/autumn 2012 (mornings when the sun was shining in a certain direction and there were dominant easterly winds); thus, corresponding T and S were removed. The C-cell is coated with antifouling spray before deployment, but, in practice, it works for only one to two months, and we find that applying the spray can increase the measured conductivity with a bias in S on the order of 0.01 psu.

We tethered Surpact to a mooring or a 15 m drogued Surface Velocity Program (SVP) drifter with a nearly buoyant line greater than 8 m long tied to the ring in front of the circular float (Figure 1). We find that Surpact usually remains nearly upwind from the drifter/mooring (there was one exception out of eight observed situations). This position means that the gimbaled axis is perpendicular to the wind and parallel to some of the wave crests, minimizing deviations of the tag from horizontal. The line is usually loose, but it sometimes becomes taut and jerks Surpact briefly. The sudden motion creates a temporary deviation of the tag axis from the vertical. This deviation is seen in the raw accelerometer data, and it tends to contribute to a background energy level in the acceleration spectrum, which contributes most to the power spectrum at low and high frequencies (below 0.5 Hz and above 2 Hz, respectively). The energy it brings into these spectra is also expected to increase with higher sea states (more jerking motions). Because of that and the lack of sensitivity of the accelerometers used, we retain only the vertical component of acceleration and estimate spectra averaged over 15 minute periods to reduce noise (40 spectra are averaged). Based on laboratory experimentation with the instrument as well as data from a preliminary cruise in September 2011 off Brittany, the meaningful frequency range retained is between 0.2 Hz and 2.2 Hz. In practice, because of the size of the float's outer ring, the acceleration spectra are strongly damped at 2 Hz and at higher frequencies. Also, it cannot detect very long swells.

We also estimate root mean square (rms) wave heights by integrating acceleration spectra (and reporting them as heights and not accelerations), and then multiplying the derived heights by 3.7 to get significant wave height (H_s). Note that these wave height estimates do not include the longest swells because of the low-frequency cutoff.

WIND ALGORITHM

We empirically find that the slope of the acceleration spectrum contains information on the wind modulus. In the algorithm, using the highest frequency part of the spectrum that responds most rapidly to changes in wind speed may seems the best approach. However, the spectrum saturates, and its slope will not change much after a certain wind threshold as the spectrum extends to lower frequencies. Thus, for higher wind speeds, we need to consider a wider range of frequencies toward the acceleration peak frequency (the peak frequency is expected to be inversely proportional to wind speed).

Figure 2a presents an example of a change in wind speeds and associated acceleration spectra. On October 4 at 12:00 a.m., there is no energy at frequencies higher than 1 Hz and only a remnant swell at 0.25 Hz. By 12:30, a little peak appears between 1.5 and 2.0 Hz. This peak gradually becomes larger

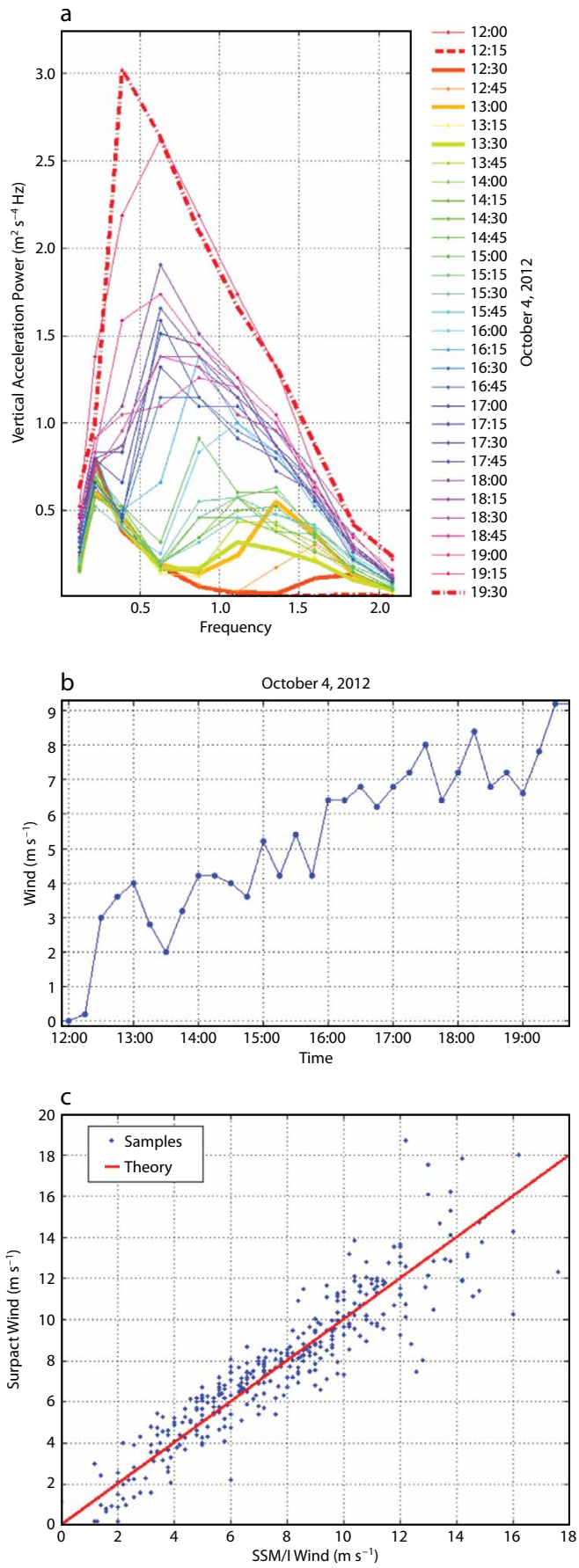

Figure 2. (a) Fifteen-minute spectra of vertical acceleration on October 4, 2012, between 12 a.m. and 7:30 p.m. (b) Estimated wind. (c) Co-location between Surpact-derived winds and SSMIS retrievals between September 9 and December 17.

and moves to lower frequencies as time passes. As this change is rather gradual, the sea should be close to full development, and the peak frequency change should indicate wind increase. There are, however, some short periods when the slope weakens in the higher part of the spectrum. We interpret these as temporary reductions in wind speed (see wind retrievals in Figure 2b based on the algorithm described below).

To develop the algorithm, we co-locate SSMIS F16 and F17 microwave wind estimates (Wentz, 1997) with the Surpact float 30798 data (September 9 to December 17, 2012). SSMIS retrievals, available at http://www.remss.com, have proven to be good indicators of wind speeds with respect to the moving surface (Mears et al., 2001) in a wide range of wind intensities, from 2 m s^{-1} to over 20 m s^{-1}. For each spectral range (i) (2 Hz > f > f_i), we consider the scatter plot of the spectral slope of vertical acceleration versus wind to determine a cutoff in wind intensity $V_c(i)$ above which the slope does not vary linearly with the wind. For winds lower than this threshold, we determine a linear regression of the wind to slope(i) as [$Vr(i) = ri \times \text{slope}(i)$], where ri is the regression coefficient between the observed spectral slope and the winds (and one ri is defined for each spectral band i considered), which usually provides a tight fit. Afterward, we derive a wind estimate, considering each 15-minute spectrum independently. We start from the highest spectral range and iteratively proceed toward lower frequencies. If the estimated $Vr(i)$ is larger than $V_c(i)$, the retained wind $V1$ is $Vr(i-1)$; if it is smaller, we iterate toward the next spectral range ($i+1$). It is

possible that this regression will provide a wind $Vr(i)$ that is less than $Vr(i-1)$. When this first happens, we define $V2 = Vr(i-1)$, but also continue to estimate $V1$ spectrally. Finally, we compare $V1$ and $V2$ (when $V2$ can be estimated) and retain the largest of the two as the wind speed estimate. This method introduces some noise in the estimated wind, as it emphasizes small changes in the spectral slope. We estimate the standard deviation of this noise to be on the order of 0.5 m s^{-1} for wind speeds between 3 m s^{-1} and 12 m s^{-1}. If there is a sudden drop in wind speed to near 0, it is possible that we temporarily overestimate wind speed. However, we cannot depend too much on the higher frequency part of the spectrum that would more directly respond to wind speed, as jerks of the line also influence it.

Our methodology might make the wind speed estimates overdependent on SSMIS retrievals. In both SSMIS microwave radiometer data and sea state retrievals from Surpact, we should also acknowledge that the wind speed estimated at 10 m is relative to the sea surface, and that it is based on a neutral layer assumption. Mears et al. (2001) show that this assumption contributes to scatter that is much smaller than the scatter of in situ absolute winds (1.24 m s^{-1}). Possibilities for differences between the SSMIS and sea-state-derived retrievals also originate from the differences in measurements. The SSMIS is instantaneous but averaged over a satellite footprint (typically larger than 20 km for the wind), whereas the sea-state-derived value is a local 15 minute average. At 1 Hz over 15 minutes, the corresponding wave footprint is less than 1 km. Also, the sea state derivation might be delayed with respect to the actual wind change seen in the SSMIS retrievals due to the time it takes for the sea elevation spectrum to adjust to wind changes. At wind speeds higher than 12 m s^{-1}, there is a possibility of contamination by nonlocal swell/wind seas in the part of the acceleration spectrum used for wind retrievals from the Surpact data. Furthermore, these seas interact with the currents, and there are also errors in SSMIS retrievals.

Figure 2c shows the results of the comparisons during the 100-day period. They are fairly reasonable, with only five differences between the two retrievals (out of 329) larger than 2 m s^{-1} for SSMIS winds less than 12 m s^{-1}. Altogether, the standard deviation of the difference between the two retrievals increases with increasing winds. It is typically on the order of 0.85 m s^{-1} for winds between 4 and 7 m s^{-1}, and 1.4 m s^{-1} for winds between 8 and 11 m s^{-1}. Thus, a rough estimate of the error is that it equals 15% of the wind modulus. Higher winds are obviously more scattered, and the statistics are not reliable (15% of the co-locations correspond to these higher winds). Over the full 100-day time series, the retrieved winds never exceed 22 m s^{-1}, but some of the highest winds are suspicious as there weren't any reported SSMIS winds larger than 18 m s^{-1}.

Similar error ranges were obtained when comparing the Surpact winds with mooring data and other direct wind estimates in near-coastal areas, both during a cruise off Brittany in September 2011 and near the Banyuls Observatory (over 20 m sea depth and 1 km from the shore) in May 2012. However, because these comparisons were done in near-coastal regions and with slightly different Surpact designs (in particular, for the outer floating ring), the retrieval algorithms were slightly different and will not be reported here.

SURPACT DATA

Deployment Four of the Strasse Cruise

During the August to September 2012 Strasse cruise, there were four long time-series stations (two to three days long) during which four or five Surpact floats were attached to 15 m drogued SVP drifters that remained within a few kilometers of each other. Other SVP drifters were also deployed, measuring C/T near 50 cm depth: Pacific Gyre drifter 114368, which reported S at only 0.01 psu resolution, and ICM drifter 30171. Wind speeds were obtained from other instruments on the nearby R/V *Thalassa* (usually within 5 km of the drifters), including from an acoustic anemometer attached to the central mast. Wind speeds were also obtained from two anemometers on the floating platform *Ocarina*, which was specially developed to gather data for air-sea flux. *Ocarina* is a 1.5 m long by 1.5 m wide trimaran that moves with the waves. It operates without engine power, and thus the hulls were usually parallel to the waves and across the wind. *Ocarina* wind measurements from the two anemometers were located at 0.85 m and 1.4 m above sea level, and are reported at 10 m height, assuming a logarithmic profile. These two wind measurements are usually rather close. *Ocarina*'s drift on the order of 20 cm s^{-1} with respect to the other drifters was not corrected. The platform was regularly recovered and redeployed (typically after eight hours) so that the distance from

the other drifters usually remained less than 5 km. *Ocarina*, as well as another platform called "trèfle," also provided wave height and H_s from their motion packages. Because of the *Ocarina*'s shape, this measurement is mostly sensitive to large waves (4 m or larger, thus periods higher than 1 s), and numbers reported are preliminary estimates.

Figure 3a compares winds recorded during the fourth Surpact deployment from September 6 to 9. Surpact sampled weak to moderate wind speeds from less than 2 m s^{-1} to 8 m s^{-1}. The wind direction was mostly from the east (except on the early morning of September 7, when it was from the east-southeast). The 15-minute winds derived from the three Surpact floats compare well, with a standard deviation between them of 0.65 m s^{-1}, compatible with the error estimate of the slope. There might be a small average difference between them, with wind estimates for 30798 a little greater (by 0.2 m s^{-1} compared to 30799). We attribute it to the tags not being perfectly identical and to differences between the accelerometers. The differences with the other wind estimates are larger, but compatible with the results provided with SSMIS. Wind differences with *Ocarina* are never larger than 2.5 m s^{-1}. There are a few instances of larger differences with the ship wind mast data, but these data are expected to be less reliable and they were collected much higher from the sea surface (near 20 m). For some reason, the ship measured stronger winds in early mornings and weaker winds for a few hours during mid-day of September 7 and 8. However, overall, the comparison is very good, giving the impression of a small lag of the sea-state-based wind retrievals compared to the other winds, except when winds are very low. This lag, which does not exceed two hours, is compatible with the time it takes for changes in the wind to be sensed at the lower frequencies for a developed sea (Romero and Melville, 2012).

H_s is also reported, but with less agreement between the different estimates

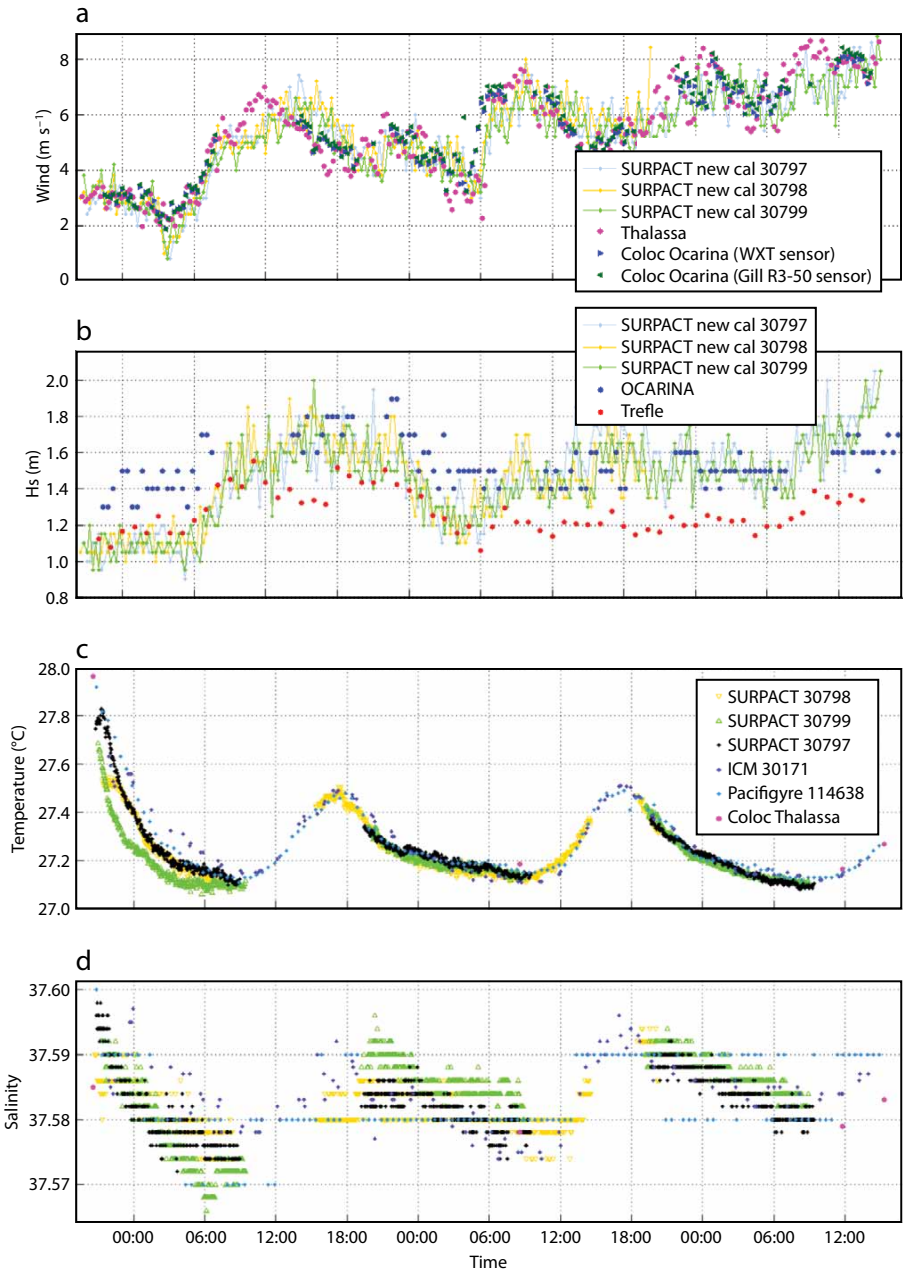

Figure 3. Strasse cruise deployment four from the evening of September 6 to the afternoon of September 9, 2012. Time is in GMT. Longitude is 35.5°W. Comparison of three Surpact measurements with nearby data. (a) Wind. (b) Significant wave height H_s from Surpact (15-minute averages), R/V *Thalassa* mast data, and data from two instruments on the *Ocarina* drifting trimaran. (c) Temperature and (d) salinity from Surpact (except in late morning), and nearby drifter data near 50 cm depth from ICM 30171 and Pacific Gyre 114638 (for salinity, the Pacific Gyre drifter sensor has 0.01 psu resolution), as well as a few nearby R/V *Thalassa* measurements near 3 m depth.

(Figure 3b). A longer swell was reported at times on September 8 and 9 that might not have contributed to the Surpact estimate. There is also the lack of the higher-frequency wave motions in the *Ocarina* and trèfle data that could result in an underestimate of their H_s toward the end when the wind picks up. Finally, it is also possible that the rate of jerking of the line attached to Surpact might result in overestimates of H_s that are sea state dependent. We tested this possibility by identifying in the vertical acceleration records all instances with strong vertical acceleration that could have been caused by the jerks, and found that they can contribute a significant part (20%) of the measured H_s, except during very low winds (4 m s^{-1} or less). In particular, removing these instances strongly reduced H_s on September 8 and 9 (to 1.2 m), more in line with the trèfle estimate. Thus, the estimates of H_s from the acceleration data are clearly not very reliable. The effect on the wind retrievals was less, except in the last hours of the deployment, when it contributed to the 1 m s^{-1} wind increase, an increase that was not registered by the anemometers.

Finally, Figure 3c,d compares temperature and salinity. During this deployment, there was usually little spatial variation in temperature and salinity. Temperatures recorded by the different drifters are rather close, except on September 6 in the evening and on the following night. During that period, there were spatial differences across the drifter patch, a remnant of the previous day's large warming. We also removed some of the Surpact data during the warming (morning) periods of September 7, 8, and 9, which indicated direct sun warming of T_c. The associated salinity presents a daily cycle in all drifters of over 0.01 psu (and close to 0.02 psu from September 6 to the morning of September 7). Peak salinity values in mid-afternoon (near 4:00 p.m. local time) coincide with highest temperatures, and the minimum salinity values in the early morning (near 6:00 a.m. local time) coincide with the lowest temperature. Measurements of T and S from samples collected by R/V *Thalassa* when it was very close to the drifters (and not on station) are consistent with these values (less so for the first point on the evening of September 6). This consistency suggests that in this period with moderate wind, the T and S daily signals are still sensed near 3 m depth, at least during nighttime/early morning. This S signal is likely related to evaporation and vertical mixing.

Examples of Observed Variability During Rainfall Events

During the 100 days after the Strasse cruise, the Surpact float attached to Pacific Gyre SVP drifter 114638 measured T and S every 30 minutes and reported five instances of significant rainfall-induced freshening. The associated wind was very variable between these rainfall event, between less than 2 m s^{-1} and more than 10 m s^{-1} (in this case, on December 3, the estimated wind peaked at 14 m s^{-1} an hour later, but the time difference might be a lag of sea states with respect to winds [see previous discussion], and thus the high wind peak might be at the onset of rain).

Figure 4 presents data for September 29, 2012, collected by both Surpact and the Pacific Gyre drifter, with rain-induced salinity drops visible at 6:00 a.m. and 6:00 p.m. (the drifter was near 26.6°N, 36.1°W in the North Atlantic subtropics). Figure 4b shows a larger initial drop in salinity at 4 cm depth (Surpact data) than at the near 50 cm depth of the Pacific Gyre drifter's sensors, which is expected during the first half hour of rainfall in the wet tropics (Reverdin et al., 2012). These two rainfall events are also associated with a

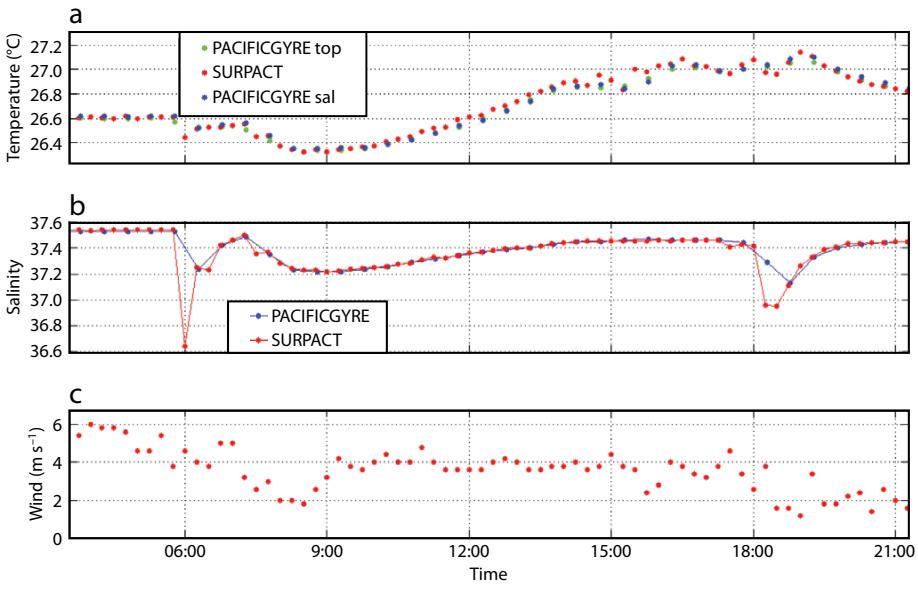

Figure 4. (a) Temperature and (b) salinity from Surpact 30798 and attached Pacific Gyre SVP drifter 114638 on September 29, 2012. (c) Estimated wind speeds (time in GMT).

temperature drop. In addition, there is a weaker drop in T and S from about 7:30 to 9:00 a.m., which could be associated with local rainfall, but could also correspond to the crossing of a small surface front or a diluted fresh puddle. This small T and S drop is associated with relatively weak winds (4 m s^{-1} for the first one at 6:00 a.m. and 2 m s^{-1} for the second one at 6:00 p.m.), which suggests slightly weaker winds during the rain. We expect this diminution is real, but there could also be damping of the sea by raindrops at the high-frequency end of the acceleration spectrum used in the retrieval (Zhang and Zhang, 2012). This contrasts with peak winds in two other salinity drop instances associated with rainfall: on December 3, as or slightly after rain began, and at the beginning of the November 22 event (on the other hand, near the end of this rainfall-induced salinity drop, wind is weak).

> "THE DATA COLLECTED BY SURPACT WILL ALLOW INSIGHT INTO THE AIR-SEA DYNAMICS OF HALINE EVOLUTION VERY CLOSE TO THE SEA SURFACE AND PROVIDE BETTER GROUND TRUTHING OF SALINITY DERIVED FROM SATELLITE RADIOMETER MEASUREMENTS."

CONCLUSIONS

We developed a "budget" floating prototype, Surpact, for measuring sea state (these data are also used to estimate wind speeds) as well as T and S 4–5 cm below the sea surface. Surpact is small in order to minimize perturbation of the flow passing through the T/C cell and to facilitate following gravity waves at 2 Hz and lower frequencies. This wave rider lasts about four months. The derivation of wind speed from the vertical acceleration spectrum proved to be robust and consistent with the error budget of SSMIS retrievals, at least for winds less than 12 m s^{-1}. Because it is an estimate derived from sea state, it tends to lag actual changes in the winds (at least for moderate or strong winds). In an oceanographic way, this is welcome as it better fits the transfer of momentum to the ocean by breaking waves (e.g., see the lag in setting Stokes drift, as noted by Ardhuin et al. [2009] or in forming breaking waves [Romero et al., 2012]). It would have been valuable to measure sea level fluctuations at higher frequencies, which we attempted with a Keller pressure sensor, but its sensitivity and response time characteristics as well as the float design proved inadequate for sensing fluctuations in the range of 2 to 10 Hz that would have been more appropriate for measuring the wind directly. Comparison of these estimates with more sophisticated current or GPS-derived wave estimates, which can be directional, made on other drifters (Peter Niiler and Luca Centurioni, Scripps Institution of Oceanography, *pers. comm.*, 2010) or wave riders (Herbers et al., 2012) would be very valuable.

Wind/wave direction is not yet measurable, but this could be implemented reasonably well in a towed model by measuring the orientation of the tag, which we found more commonly down wind from the attached drifter (except in one instance on the afternoon of September 8 during the Strasse cruise in which the current was rotating between 15 m and the surface in such a way as to bring the float very close to the drifter despite an established sea).

The C/T measurements were reasonably accurate, at least for the first two months. The sensitivity of the T_c measurement to direct warming of the tag's side faces by the sun should easily be corrected by painting the sides with reflecting paint, as is done to the top surface. The conductivity measurement from the Valport conductivity cell suffers from fouling. It is very difficult to protect an open inductive sensor from fouling. Other simple and small C/T sensors could be considered to improve this measurement and make it more affordable. Furthermore, it would be interesting to implement a simple acoustic noise measurement under the cover of the SLP sensor on top of the tag to investigate rainfall rate. We will also need to better estimate the flow around the C and T sensors to attribute a depth or depth range from the sea surface to these measurements. Preliminary tank tests suggest that the current design could mix the upper 5–10 cm layer when Surpact

is attached to an SVP drifter, even with very weak winds (the tests were conducted towing Surpact at 10 cm s^{-1}).

ACKNOWLEDGMENTS

This effort is part of ESA SMOS cal-val projects, and is supported nationally in France by CNES/TOSCA with the Gloscal project, and in Spain at ICM/CSIC by the Spanish national R+D plan (project AYA2010-22062-C05). Support from SMRU for development of the Surpact tag and from the crew of R/V *Thalassa* during the sea trials is gratefully acknowledged. The Strasse/SPURS cruise was also funded by INSU, and the development of *Ocarina* and Surpact by IPSL. The cruise took place on board R/V *Thalassa* owned by Ifremer and operated by GENAVIR. SSMIS data are produced by Remote Sensing Systems and sponsored by the NASA Earth Science MEaSUREs DISCOVER Project. One of the authors, Gilles Reverdin, is strongly indebted to P.P. Niiler's contagious enthusiasm about the use of drifters, which he first communicated to him during a meeting in 1981, when, as a young scientist unaccustomed to such venues, he was a bit at a loss.

REFERENCES

Ardhuin, F., L. Marié, N. Raszcle, P. Forget, and A. Roland. 2009. Observation and estimation of Lagrangian, Stokes, and Eulerian currents induced by wind and waves at the sea surface. *Journal of Physical Oceanography* 39:2,820–2,838, http://dx.doi.org/10.1175/2009JPO4169.1.

Bingham, F.M., S.D. Howden, and C.J. Koblinsky. 2002. Sea surface salinity measurements in the historical database. *Journal of Geophysical Research* 107, 8019, http://dx.doi.org/10.1029/2000JC000767.

Bingham, F.M., G.R. Foltz, and M.J. McPhaden. 2010. Seasonal cycles of surface layer salinity in the Pacific Ocean. *Ocean Science* 6:775–787, http://dx.doi.org/10.5194/os-6-775-2010.

Bingham, F.M., G.R. Foltz, and M.J. McPhaden. 2012. Characteristics of the seasonal cycle of surface layer salinity in the global ocean. *Ocean Science* 8:915–929, http://dx.doi.org/10.5194/os-8-915-2012.

Boutin, J., N. Martin, G. Reverdin, and X. Xin. 2012. Sea surface freshening inferred from SMOS and ARGO salinity: Impact of rain. *Ocean Science* 9:3,331–3,357, http://dx.doi.org/10.5194/osd-9-3331-2012.

Cravatte, S., T. Delcroix, D. Zhang, M. McPhaden, and J. LeLoup. 2009. Observed freshening and warming of the western Pacific warm pool. *Climate Dynamics* 33:565–589, http://dx.doi.org/10.1007/s00382-009-0526-7.

Cronin, M.F., and M.J. McPhaden. 1999. Diurnal cycle of rainfall and surface salinity in the western Pacific warm pool. *Geophysical Research Letters* 26:3,465–3,468.

Foltz, G.R., and M.J. McPhaden. 2008. Seasonal mixed layer salinity balance of the tropical North Atlantic Ocean. *Journal of Geophysical Research* 113, C02013, http://dx.doi.org/10.1029/2007JC004178.

Font, J., A. Camps, A. Borges, M. Martin-Neira, J. Boutin, N. Reul, Y. Kerr, A. Hahne, and S. Mecklenburg. 2010. SMOS: The challenging sea surface salinity measurements from space. *Proceedings of the IEEE* 98(5):649–665, http://dx.doi.org/10.1109/JPROC.2009.2033096.

Font, J., J. Boutin, N. Reul, P. Spurgeon, J. Ballabrera-Poy, A. Chuprin, C. Gabarro, J. Gourrion, S. Guimbard, C. Hénocq, and others. 2013. SMOS first data analysis for sea surface salinity determination. *International Journal of Remote Sensing* 34:3,654–3,670, http://dx.doi.org/10.1080/01431161.2012.716541.

Hénocq, C., J. Boutin, G. Reverdin, F. Petitcolin, S. Arnault, and P. Lattes. 2010. Vertical variability of near-surface salinity in the tropics: Consequences for L-Band radiometer calibration and validation. *Journal of Atmospheric and Oceanic Technology* 27:192–209, http://dx.doi.org/10.1175/2009JTECHO670.1.

Herbers, T.H.C., P.F. Jessen, T.T. Janssen, D.B. Colbert, and J.H. MacMahan. 2012. Observing ocean surface waves with GPS-tracked buoys. *Journal of Atmospheric and Oceanic Technology* 29:944–959, http://dx.doi.org/10.1175/JTECH-D-11-00128.1.

Lagerloef, G., F. Wentz, S. Yueh, H.-Y. Kao, G.C. Johnson, and J.M. Lyman. 2012. State of the climate in 2011: Aquarius satellite mission provides new, detailed view of sea surface salinity. *Bulletin of the American Meteorological Society* 93(7):S70–S71.

Mears, C.A., D.K. Smith, and F.J. Wentz. 2001. Comparison of Special Sensor Microwave Imager and buoy-measured wind speeds from 1987–1997. *Journal of Geophysical Research* 106:11,719–11,729, http://dx.doi.org/10.1029/1999JC000097.

Reverdin, G., P. Blouch, J. Boutin, P. Niiler, J. Rolland, W. Scuba, A. Lourenço, and A. Rios. 2007. Surface salinity measurements—COSMOS 2005 experiment in the Bay of Biscay. *Journal of Atmospheric and Oceanic Technology* 24:1,643–1,654, http://dx.doi.org/10.1175/JTECH2079.1.

Reverdin, G. 2010. North Atlantic subpolar gyre surface variability (1895–2009). *Journal of Climate* 23:4,571–4,584, http://dx.doi.org/10.1175/2010JCLI3493.1.

Reverdin, G., S. Morrisset, J. Boutin, and N. Martin, 2012. Rain-induced variability of near sea-surface T and S from drifter data. *Journal of Geophysical Research* 117, C2, http://dx.doi.org/10.1029/2011JC007549.

Romero, L., W.K. Melville, and J.M. Kleiss. 2012. Spectral energy dissipation due to surface wave breaking. *Journal of Physical Oceanography* 42:1,421–1,444, http://dx.doi.org/10.1175/JPO-D-11-072.1.

Roquet, F., J.-B. Charrassin, S. Marchand, L. Boehme, M. Fedak, G. Reverdin, and C. Guinet. 2011. Delayed-mode calibration of hydrographic data obtained from animal-borne satellite relay data loggers. *Journal of Atmospheric and Oceanic Technology* 28(6):787–801, http://dx.doi.org/10.1175/2010JTECHO801.1.

Schmitt, R.W. 2008. Salinity and the global water cycle. *Oceanography* 21(1):12–19, http://dx.doi.org/10.5670/oceanog.2008.63.

Singh, A., and T. Delcroix. 2011. Estimating the effects of ENSO upon the observed freshening trends of the western tropical Pacific Ocean. *Geophysical Research Letters* 116, C06016, http://dx.doi.org/10.1029/2011GL049636.

Swift, C.T. 1980. Passive microwave remote sensing of the ocean: A review. *Boundary-Layer Meteorology* 18:25–54, http://dx.doi.org/10.1007/BF00117909.

Wentz, F. 1997. A well-calibrated ocean algorithm for special sensor microwave/imager. *Journal of Geophysical Research* 102:8,703–8,718, http://dx.doi.org/10.1029/96JC01751.

Yu, L. 2010. On sea surface salinity skin effect induced by evaporation and implications for remote sensing of ocean salinity. *Journal of Physical Oceanography* 40:85–102, http://dx.doi.org/10.1175/2009JPO4168.1.

Yu, L. 2011. A global relationship between the ocean water cycle and near-surface salinity. *Journal of Geophysical Research* 116, C10025, http://dx.doi.org/10.1029/2010JC006937.

Zhang, Y., and X. Zhang. 2012. Ocean haline skin layer and turbulent surface convections. *Journal of Geophysical Research* 117, C04017, http://dx.doi.org/10.1029/2011JC007464.